Springer

KSME

Journal of Mechanical Science and Technology 30 (12) (2016) 5817~5828
www.springerlink.com/content/1738-494x(Print)/1976-3824(Online)
DOI 10.1007/s12206-016-1152-z

Development of a program for transient behavior simulation of heavy-duty gas turbines †

Jeong Ho Kim[1], Tong Seop Kim[2,*] and Seung Jae Moon[3]

[1]*Graduate School, Inha University, Incheon 22212, Korea*
[2]*Dept. of Mechanical Engineering, Inha University, Incheon 22212, Korea*
[3]*Dept. of Mechanical Engineering, Hanyang University, Seoul 04763, Korea*

(Manuscript Received May 17, 2016; Revised July 25, 2016; Accepted September 12, 2016)

Abstract

In this study, a program for analyzing the transient behaviors of heavy-duty gas turbines was developed. Focus was given to simulating a practical load-following operation. A distinct feature of our work is that all of the gas turbine components are modularized to enhance the expandability of the program. We used object-oriented programing for this purpose. Mass and energy balances and performance maps for the compressor and turbine were used for the modeling, and a multivariable numerical solving technique was used to enhance the numerical stability. The fundamental thermodynamic modeling of the program was validated by comparison of the transient response of a simulated gas turbine with that of a commercial program. PID control was adopted for simultaneous control of the rotational shaft speed and turbine exhaust temperature by the modulations of the fuel flow and the opening of the compressor inlet guide vane at the same time. The influence of the magnitude of load change and ramp rate was investigated. Stable control of the gas turbine was possible, even for a very rapid change of load.

Keywords: Gas turbine; Transient behavior; Simulation; Control; Load profile

1. Introduction

Gas turbine technology has developed remarkably since its full-scale introduction to the electric power generation market in the 1980s, and it is now one of the main sources of power. Gas turbines have future prospects in the forthcoming age of renewable energy due to their various advantages over other technologies, such as steam turbine plants powered by fossil fuels (mostly coal). The major renewable technologies such as solar and wind power have a critical drawback of intermittent power generation. Owing to the advantage of swift power change, the gas turbine is the most reliable power source that can rapidly back up the electric grid in response to the fluctuating power generation of renewable sources [1].

The demand for gas turbines and the gas/steam-turbine combined cycle is expected to remain high in the future. However, even faster responses to changes in electric load will eventually be required from the electricity market. Such a market demand will bring about the need for further technology developments in future gas turbines. Research and development are needed to ensure stable operation in the rapidly changing working conditions.

*Corresponding author. Tel.: +82 32 860 7307, Fax.: +82 32 868 1716
E-mail address: kts@inha.ac.kr
† Recommended by Associate Editor Jae Dong Chung

When the power supply of an electrical grid becomes unstable, a gas turbine rapidly performs a load change (acceleration and deceleration) to resolve the situation. This rapid load change or repetitive extreme conditions such as start-up and shut-down can damage the gas turbine. A rapid load change damages the hot part of the gas turbine (the turbine blades) and the heat recovery steam generator of combined cycle power plants. Frequent changes in working conditions of the critical components decrease their lifetimes and raise safety issues for the entire power plant. Therefore, to avoid extreme conditions, precise prediction of the transient state change inside every component in the early stages of gas turbine development is very important. An optimized operation scheme enabled by precise prediction will contribute to a more stable and swift load change of the developed gas turbine.

Methods for analyzing the transient behaviors involve either an experiment or an analysis through simulation. In the case of experiments, relatively accurate behavior analysis is possible, but there are numerous limitations regarding time and costs. Therefore, simulation is generally preferred. However, the results of simulation depend on the analysis models. There have been various efforts to enhance the simulation accuracy. Some recent works compared the dynamic behaviors of an actual power plant and those predicted by commercial programs with different analysis models [2, 3]. There have also

been efforts to increase the expandability of programs via object-oriented simulation [4, 5]. One study analyzed the dynamic behaviors of a gas turbine using the nonlinear autoregressive exogenous (NARX) model [6].

The major commercial programs used for performance analysis of gas turbines are GasTurb [7], GateCycle [8], GSP [9], PROOSIS [10], ProTRAX [11] and NPSS [12], and gas turbine performance can be analyzed by selecting premanufactured components with the program interface. To stably assist users with fewer specialties, some commercial programs limit their access to the mathematical models. This might be useful for a non-professional conducting gas turbine performance analysis. However, this also means that the scope of the performance analysis can be limited, and it is difficult for the user to analyze various types of system configurations. Cases might occur where the system is very complex or the users are required to modify the source code for the model. To resolve these limits, programs based on object-oriented languages such as GSP and PROOSIS were developed [4]. Such languages enhance the reusability, expandability, and modularization of the code, and a user can model various types of gas turbines more easily.

All of the commercial programs mentioned above provide user-defined component modeling to some extent. However, each program focuses on different features, and the various user demands cannot all be fully satisfied. A simple example is the fuel choices. Natural gas is the reference fuel for gas turbines, but many recent studies are investigating biogas or syngas as new fuels. For example, some studies examined the Integrated gasification combined cycle (IGCC) using syngas [13, 14], a gas turbine combined heat and power system that uses biogas [15], and a micro gas turbine that uses biogas [16].

Transient operation includes changes in rotor speed, volume packing, heat soakage, and time lag of the control system [17]. The accuracy of the analysis depends on the capability of modeling these factors, and the commercial programs differ widely in the detailed modeling. Consideration is required for the suitability of the component modeling for a specific analysis purpose. Some commercial programs calculate the performance of gas turbines by using the choking condition of the turbine. Heavy-duty gas turbines are mainly operated in the choking condition in normal operation near the design points. However, in the case of start-up or rapid load change, a turbine performance map should be used to ensure accurate analysis.

Our ultimate research goal is to develop an in-house dynamic simulation program capable of simulating full dynamic operations including load-following transient operations as well as full start-up and shut-down procedures. As a first step of this long-term development project, we set up the modeling of the load-following simulation and this paper presents the program modeling and results. The developed program mainly focuses on the simulation of dynamic behaviors similar to those of a real engine in a wide operation range.

The program is capable of analyzing both steady state and dynamic behaviors. Compressor and turbine performance maps are used, and a turbine blade cooling model is incorporated. Various types of gaseous fuel can be used. The fuel flow rate and the opening of the compressor Inlet guide vane (IGV) can be modulated simultaneously to control the shaft speed and the Turbine exhaust temperature (TET). The simulation considers the time lag of the control system that occurs when controlling the fuel flow rate and the IGV angle. The results of the program were validated using commercial programs, and the dynamic behavior change of the gas turbine was analyzed in accordance with the load profile.

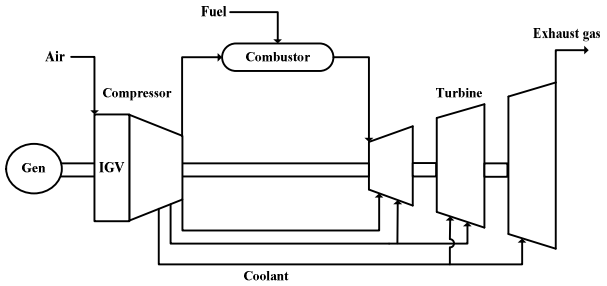

Fig. 1. System configuration.

2. Modeling

2.1 Overview

The program was developed using MathWorks MATLAB [18]. Each component of the gas turbine was modularized by applying object-oriented programming, which increased the expandability and reusability. The configuration of the heavy-duty gas turbine for power generation is shown in Fig. 1. Our current focus is on the single-shaft simple-cycle engine shown in the figure, but our application can be expanded easily to various types of gas turbines in the future due to the object-oriented programming.

The governing equation of the rotor shaft is given by Eq. (1).

$$I\frac{d\omega}{dt} = (\dot{W}_{net} - \dot{W}_{load}) / (N \times \frac{2\pi}{60}) . \quad (1)$$

The rotational speed of the shaft changes in transient conditions due to the imbalance between the net shaft power output and the load. In the load-following operation, an external load is the input of the simulation, while the power output response and the resulting rotational speed are the simulation outputs.

The entire gas turbine is modeled as a sum of several control volumes (components such as the compressor combustor, turbine, ducts, and so on), which satisfy mass and energy equations. The fluid speed is far higher than the rate of the rotational speed change, so each control volume is assumed to be in thermodynamic equilibrium in every time step [19, 20]. Thus, the fluid inertia in the mass and energy equations was ignored, and a quasi-steady state model was used.

2.2 Properties

There are two options in the program for calculating the working fluid properties: ideal gas properties using temperature-dependent specific heat data, or real gas properties using REFPROP [21]. With ideal gas properties, the enthalpy and entropy at any location are calculated using the ideal gas mixing rule and constant pressure specific heat data for each gas composition [22]. The humidity of the ambient air was taken into account using the water vapor pressure correlation.

2.3 Compressor

Every modern heavy-duty gas turbine uses a multi-stage axial compressor, and a portion of air is bled at several interstages and fed to the turbine to cool the turbine blades. The exact amount of coolant bled from each location in commercial gas turbines is hard to estimate precisely. However, the entire amount of coolant and the first-stage nozzle coolant can be calculated using information about the Turbine inlet temperature (TIT) and Turbine rotor inlet temperature (TRIT, temperature at the first stage rotor inlet). The coolant of the turbine rows after the first-stage nozzle rotor was estimated using available information from previous research, such as the coolant distribution [23]. In off-design and transient operation, the coolant distribution is assumed to be the same as in the design conditions. If the pressure ratios of all stages are given, we can simply input them. Otherwise, we assume that the pressure ratio is equally distributed in all stages.

The outlet enthalpy of each stage is calculated using the stage efficiency as in the following equation, which also provides the temperature and pressure of the turbine cooling air.

$$\eta_{comp,st} = \frac{h_{out,st,s} - h_{in,st}}{h_{out,st} - h_{in,st}} . \quad (2)$$

The power consumption of the compressor is then calculated as the sum of the power consumption of each stage.

$$\dot{W}_{comp} = \sum_{i=1}^{n_{comp}} \left[\dot{m}_{air,in} \times (h_{out,st} - h_{in,st}) \right]_i . \quad (3)$$

The compressor performance map used in the simulation is shown in Fig. 2. It describes relationships among dimensionless speed and mass flow ($N/\sqrt{T_{in}}$, $\dot{m}\sqrt{T_{in}}/P_{in}$), pressure ratio and efficiency. The β-lines are arbitrary lines that facilitate map interpolation and were used to find the operating point on the performance map [24]. At high rotational speed, there is a zone where the flow rate effectively does not change (i.e., the flow is choked) with changes in pressure ratio. Because the constant speed line is vertical in the zone, the pressure ratio cannot be determined. To resolve this problem, the β-lines are used. When the operating point is determined in the performance map, the flow rate, pressure ratio, and efficiency are also determined.

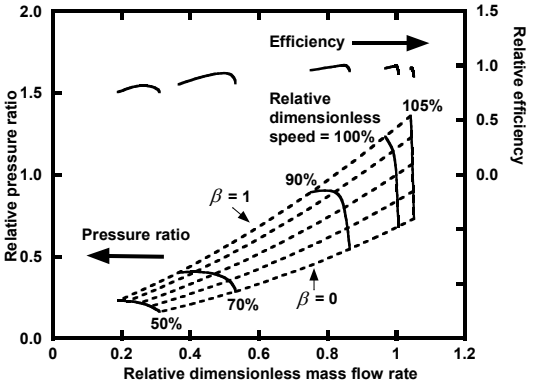

Fig. 2. Compressor performance map.

In the case of a heavy-duty gas turbine, the rotor shaft should be controlled to maintain a constant speed during all operations. The turbine exhaust temperature is also controlled to maintain as high a value as possible. This is usually done to provide a high partial load efficiency for combined cycle power plants. To control the turbine exhaust temperature, the IGV angle is adjusted to modulate the mass flow rate through the compressor. The shape of the performance map changes when the mass flow rate changes as a result of the IGV angle adjustment. The changes in the shape of the compressor performance map are simulated according to the IGV angle. This is done by multiplying the mass flow rate and pressure ratio by the scaling factors regarding the IGV angles defined by the following equation:

$$\dot{m}_{sc} = \dot{m}_o \times sf_{IGV} , \quad PR_{sc} = PR_o \times sf_{IGV} . \quad (4)$$

2.4 Combustor

Complete combustion is assumed [25]. A wide range of gaseous fuels (natural gas, syngas, biogas, etc.) can be simulated because the fuel composition can be selected by the user. In the design calculation, an exact amount of fuel supply is calculated to achieve the target performance of the gas turbine (net power and efficiency). In off-design and transient analyses, the fuel supply is controlled to match the net power output to the required load.

2.5 Turbine

A stage-by-stage calculation was used in our turbine modeling. Cooling of the hot sections, (especially turbine blades) is important because gas turbines are operated at high temperatures for a long time. Therefore, to accurately simulate the performance of a heavy-duty gas turbine, turbine cooling modeling must be conducted. However, accurate modeling of the turbine cooling for commercial engines is difficult because there is little information about the details of the cooling schemes. A number of turbine cooling models have been sug-

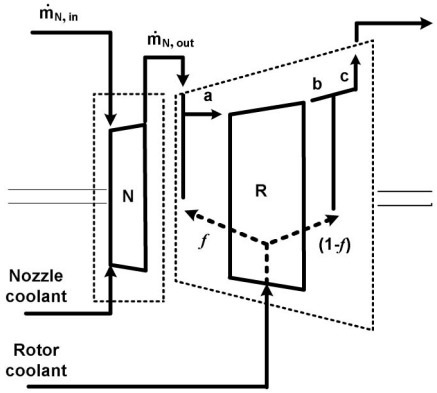

Fig. 3. Turbine cooling modeling.

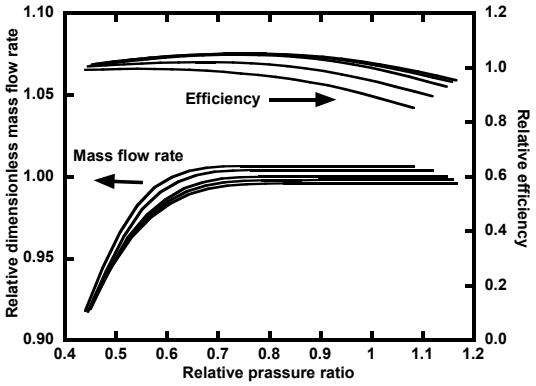

Fig. 4. Turbine performance map.

gested, with various advantages and disadvantages. The cooled turbine stage model in Fig. 3 was used in our program.

Coolant is bled from the inter-stages of the compressor and used for cooling the nozzles and rotors of the turbine. The power output is generated by the expansion of fluid in the rotor. All the coolant of the nozzle and a portion of the coolant of the rotor (*f*) contribute to the turbine output produced by the rotor. The fluid expands from the rotor inlet Fig. 3(a) to the rotor outlet Fig. 3(b). The coolant (1-*f*) that does not contribute to the power output is mixed at the rotor outlet and becomes a final-stage outlet condition Fig. 3(c).

The stage efficiency and the turbine power output, which is the sum of all stage outputs, are defined by the following equations:

$$\eta_{turb,st} = \frac{h_a - h_b}{h_a - h_{b,s}} \tag{5}$$

$$\dot{W}_{turb} = \sum_{i=1}^{n_{nuth}} \left[(\dot{m}_{in,N} + \dot{m}_{C,N} + \dot{m}_{C,f}) \times (h_a - h_b) \right]_i . \tag{6}$$

The pressure ratio and efficiency of each stage can be individually specified as calculation inputs. We assumed an equal pressure ratio distribution and an identical efficiency in our sample calculation.

Our cooled stage model is similar to the cooling model of GateCycle [8]. The detailed equations of the GateCycle model were not available, but the factor *f* is similarly defined. We performed calculations for arbitrary cooled turbine stages using the same *f* and stage efficiency in both our program and GateCycle, which showed very close values. This confirmed that our turbine model is at least as feasible as that of the commercial program. The factor *f* is set as 0.5 in our sample calculation.

Fig. 4 shows the turbine map used for our calculation. The β-lines in the turbine map are used for the easiness of map interpolation as we did for the compressor map. Matching between the compressor and turbine maps determines an operating point. It was assumed that the stage expansion ratio distribution and efficiencies of all stages are the same as in the design calculation.

The method so far is based on the fact that a turbine map is available. If a turbine map is not available, the turbine off-design model is replaced by the choking equation [26]:

$$\frac{\dot{m}_{\text{in}}\sqrt{T_{\text{in}}}}{\kappa A P_{\text{in}}} = \text{constant, where } \kappa = \sqrt{\frac{\gamma}{R}\left(\frac{2}{\gamma+1}\right)^{\frac{\gamma+1}{\gamma-1}}} . \tag{7}$$

The design points of modern gas turbines are close to a choked condition. Therefore, this method is feasible for industrial gas turbines as long as the turbine expansion ratio does not deviate much from the design value. The turbine output calculation is the same as in the map-based method (Eq. (10)), but the stage efficiency is corrected using an analytical method [27]:

$$\frac{\eta_{turb,st}}{\eta_{turb,st,d}} = \frac{N}{N_d}\sqrt{\frac{\Delta h_{s,d}}{\Delta h_s}}\left[2 - \frac{N}{N_d}\sqrt{\frac{\Delta h_{s,d}}{\Delta h_s}}\right] . \tag{8}$$

There are limits for using the choking condition, especially when the operating expansion ratio is quite low as in the start-up operation. Therefore, using a turbine map is preferred for the expandability of our program.

2.6 Inlet and exhaust ducts

Ducts are used for connecting any two components. The pressure loss is assigned in the design point analysis, while in the off-design analysis, the pressure loss is corrected using the following equation [28]:

$$\frac{(\Delta P / P_{in})}{(\Delta P / P_{in})_d} = \frac{(\dot{m}\sqrt{T} / P_{in})^2}{(\dot{m}\sqrt{T} / P_{in})_d^2} \times \frac{R}{R_d} . \tag{9}$$

2.7 Control unit

Heavy-duty commercial gas turbines are not always oper-

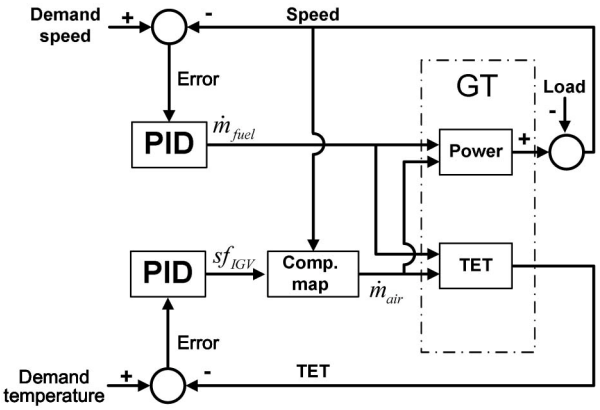

Fig. 5. Schematic diagram of control block.

ated in the steady state. Controlling gas turbines is important to prevent surges due to unexpected load changes or fuel supply problems and to prevent abrupt increases in the rotational speed and turbine inlet temperatures. A PID control method was used to stably control a gas turbine in the transient state, as shown in Fig. 5. Similar controls based on PID logic to control both the speed (or power) and exhaust temperature have been successfully used for transient behavior simulations of large heavy duty gas turbines [29], and micro gas turbines [30, 31].

The entire control consists of two sub-control units: speed control and TET control. The manipulated variables for the former and the latter are the fuel flow rate and the IGV factor, respectively. When the rotational speed increases or decreases because of a load change, the fuel is controlled to maintain the rotational speed. In the case of partial-load gas turbine operation in combined cycle power generation, the turbine exhaust temperature is controlled to maintain the maximum output generated from the bottoming cycle. To control the turbine exhaust temperature, the compressor inlet air flow is controlled by changing the IGV factor. The two sub-control units do not operate independently from each other but are cross-coupled. The output parameter of each control unit affects the input parameter of the other as depicted by the connecting lines between the two controls. The speed control causes a variation in TET through the changes in firing temperature and compressor air flow rate, and the air flow rate controlled by the TET control affects the fuel flow rate.

As shown in Fig. 5, the fuel flow rate and IGV factor should be controlled simultaneously. The equation of the PID control is shown below. The optimized proportional coefficient, integrated coefficient, and differential coefficient were estimated by trial and error. A case study for determining the coefficient is presented in Sec. 3.3.

$$X(t+1) = X(t) + K_P e(t) + K_I \int_0^t e(t)dt + K_D \frac{de(t)}{dt}. \quad (10)$$

In real gas turbines, components such as the IGV and fuel valve are usually relocated by the control unit during the transient conditions. Each component is operated by an actuator, which has an intrinsic delay usually called actuator delay in the response to the command of the control unit. This delay is usually referred to as time lag and is simulated using the following equation [17]:

$$X_{metered}(t+dt) = \frac{(X_{metered}(t) \times TC) + (X_{demanded}(t+dt) \times dt)}{(TC + dt)}. \quad (11)$$

The actual fuel flow rate in the next time step is calculated using the demanded fuel supply and the fuel flow rate measured in the current time step in consideration of the time lag. It is known that the actuator delay usually increases control instability. We considered the delay time by a Time constant (TC) in Eq. (11), and further confirmed that the delay time does not affect the control instability in our simulation. The exact time constant should be provided by the manufacturer of the control unit system. In this study, the time constant was set as 0.01 s [17].

2.8 Gas turbine performance

After the performance analysis, the net power and efficiency of the gas turbine are calculated as follows in consideration of the mechanical loss, generator loss, etc.:

$$\dot{W}_{net} = (\dot{W}_{turb} - \dot{W}_{comp}) \times \eta_{mech} \times \eta_{gen} \quad (12)$$

$$\eta_{net} = \frac{\dot{W}_{net}}{(\dot{m} \times LHV)_{fuel}}. \quad (13)$$

2.9 Program structure

The structure of our program is shown in Fig. 6. A steady state analysis should be performed before dynamic analysis. The design point analysis is performed with the ISO standard conditions (288.15 K, 1 atm, 60 % relative humidity) using the input variables of the input data module. The dynamic calculation is closely related to the off-design calculation routine, which includes all of the essential off-design characteristic models of all components. The performance maps of the compressor and turbine and the results of the design point calculation are used for the off-design calculation. An operating point that satisfies the mass and energy conservation was thus calculated. This process is called matching between components, especially those between the compressor and the turbine. The multi-dimensional Newton–Raphson method was used to solve the complex equation sets [32]. The dynamic calculation is carried out with the shaft torque balance equation, the controller model, and the load input patterns.

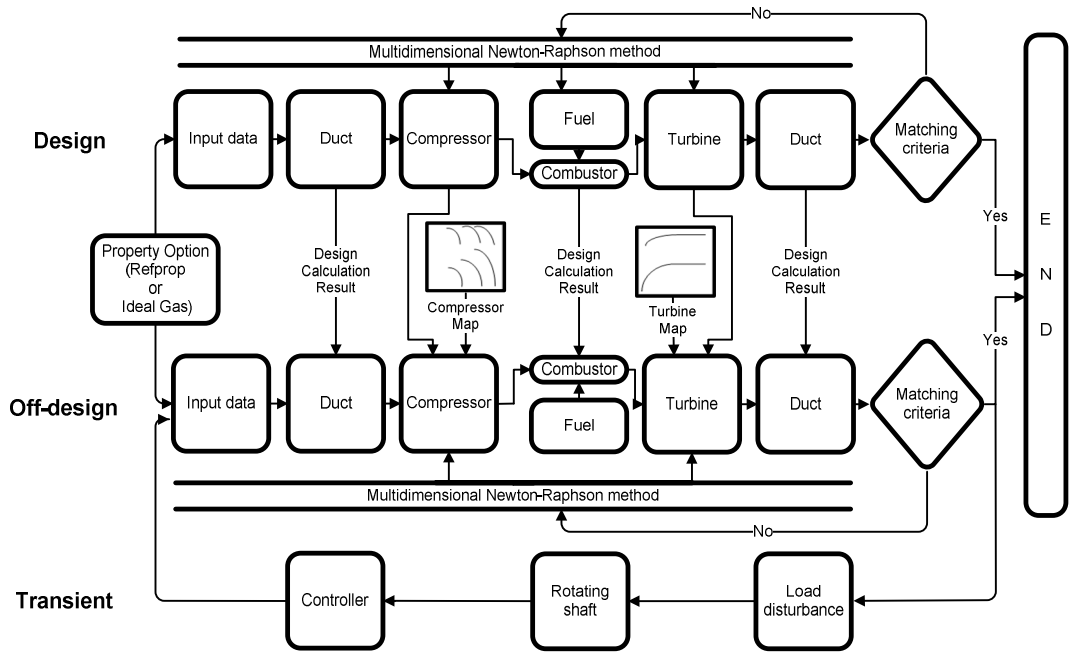

Fig. 6. Program structure.

3. Results and discussion

3.1 Steady state validation

The program was validated by simulating the General electric (GE) 7FA, which is one of the most widely used commercial gas turbines. Prior to the transient analysis, the basics of the thermodynamic modeling were validated using steady state simulation. The design point performance was simulated with our program, GateCycle [8] and PROOSIS [10], and the results of three programs were compared. The design specifications from the manufacturer [33, 34] and simulation results are compared in Table 1. The fuel is natural gas, and its composition and low heating value are shown in Table 2. The component characteristic parameters such as the efficiencies of the compressor and turbine were not provided by the manufacturers. Thus, appropriate values satisfying the design power output and efficiency were estimated.

The known turbine inlet temperature, turbine rotor inlet temperature, and turbine exhaust temperature were used to estimate the turbine coolant flow rate and stage efficiency. Table 3 shows the cooled turbine locations, coolant extraction locations, coolant flow rates, and temperatures. The coolant flow rates were determined by our in-house program, and the same values were assigned in the other commercial programs. The resulting coolant temperatures are slightly different among the three programs. The coolant temperatures of our program and GateCycle are quite close, even though GateCycle uses a different thermodynamic database [35]. This means that the two property databases provide almost the same results.

PROOSIS uses the same thermodynamic database as GateCycle. Therefore, the slightly larger deviations of its results from those of other two programs are due to the difference in calculating the coolant properties. In GateCycle and our program, a stage-by-stage calculation naturally produces the coolant temperatures. However, PROOSIS uses a unique method of estimating coolant temperatures with a factor that determines the enthalpy of the coolant source [10]. The comparison in Table 1 shows that all of the gas turbine performance parameters (power output, efficiency, and turbine exhaust temperature) simulated by our program match the data provided by manufacturers very well (within 0.3 %). The entire coolant rate was expected to be 17.83 % of the inlet air mass flow rate.

Off-design analyses were performed as a second step of the validation of the steady state modeling, and the results were compared with available manufacturer data. The compressor and turbine performance maps used in our calculation (Figs. 2 and 4) were taken from the PROOSIS database. They differ from those of the actual engine (7FA), so they were scaled to reproduce the performance correction curves of the engine provided by GE [36] sufficiently well. Fig. 7 shows the predicted performance variation with ambient temperature at full load conditions, where the turbine rotor inlet temperature is maintained at the design value. There was good agreement between the prediction and manufacturer data.

Fig. 8 shows the partial load performance at an ambient temperature of 288.15 K. To enhance the heat recovery from the gas turbine exhaust, the turbine inlet temperature was maintained from 100 % load to 80 % partial load by controlling the IGV angle and fuel flow. After the IGV is fully closed, the power output is controlled by only the fuel flow down to 0 % load, resulting in almost constant exhaust mass flow. The results of the performance prediction and the manufacturer's

Table 1. Design specification of gas turbine.

	Parameters	Manufacturer's reference data [33, 34]	In-house program	GateCycle	PROOSIS
Inlet	Air temperature (K)	288.15	288.15	288.15	288.15
	Air pressure (kPa)	101.325	101.325	101.325	101.325
	Relative humidity (%)	60	60	60	60
	Air flow rate (kg/s)	435	435	435	435
Compressor	Pressure ratio (-)	16	16	16	16
	Stage polytropic efficiency (%)	NA	89.8	89.8	89.8
	Number of stage (-)	18	18	18	18
Combustor	Fuel flow rate (kg/s)*	NA	9.46	9.46	9.46
	Pressure loss (%)	NA	4	4	4
Turbine	Turbine inlet temperature (K)	1670.15	1670.15	1670.15	1670.15
	Turbine rotor inlet temperature (K)	1600.15	1600.15	1600.15	1600.15
	Turbine exhaust temperature (K)*	874.25	874.25	875.60	876.00
	Number of stage (-)	3	3	3	3
	Stage efficiency (%)	NA	87.8	87.8	87.8
	Total coolant fraction (%)*	NA	17.83	17.83	17.83
Duct	Pressure loss (%)	0.5	0.5	0.5	0.5
Performance	Shaft speed (rpm)	3600	3600	3600	3600
	Mechanical efficiency (%)	NA	99	99	99
	Generator efficiency (%)	NA	98.5	98.5	98.5
	GT power (MW)*	171.6	171.5	171.5	171.3
	GT efficiency (%)*	36.80	36.80	36.78	36.78

* Simulation outputs (the fuel flow rate and the total coolant fraction are simulation outputs in the in-house program but are used as input in the two commercial programs)

Table 2. Natural gas properties.

Component	Mole fraction (%)
CH_4	0.9133
C_2H_6	0.0536
C_3H_8	0.0214
C_4H_{10}	0.0095
N_2	0.0022
Lower heating value (kJ/kg)	49300.1

Table 3. Coolant properties for each cooled blade row.

Cooled turbine blade row	Coolant source (compressor stage exit)	Coolant fraction relative to compressor inlet air flow	Coolant temperature (K)		
			In-house program	Gate Cycle	PROOSIS
1st nozzle	18	7.31 %	681.72	681.87	682.72
1st rotor	17	2.87 %	652.14	651.20	653.80
2nd nozzle	13	2.39 %	543.78	540.16	554.00
2nd rotor	17	2.87 %	652.14	651.20	653.80
3rd nozzle	13	2.39 %	543.78	540.16	554.00

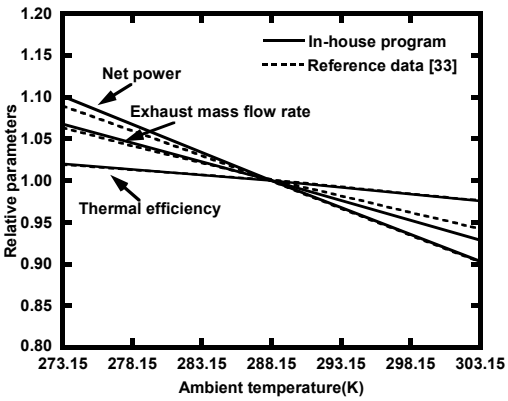

Fig. 7. Variation in full-load performance of 7FA with ambient temperature.

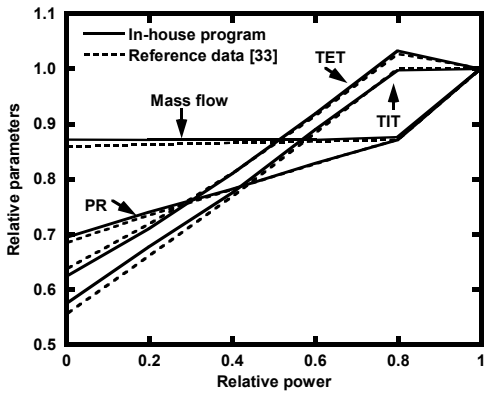

Fig. 8. Part-load performance (288.15 K ambient temperature).

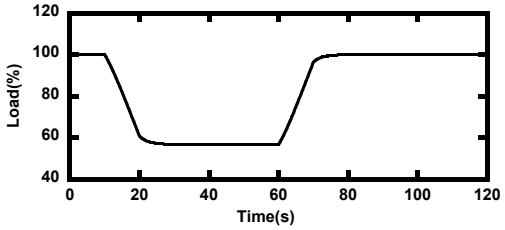

Fig. 9. Load profile.

data are very close (pressure ratio, turbine inlet temperature, turbine exhaust temperature, and exhaust mass flow rate).

The results show that all of the basic modeling of our program such as working fluid properties and component models are appropriate and sufficient for dynamic analysis.

3.2 Transient response

We also validated our program for simulation of the dynamic behavior of gas turbines. We compared results of our program with a reliable commercial program. Comparison with real operation data must be the best way to verify our program but obtaining precisely measured operation data suitable for our validation purpose was very hard. Furthermore, we obtained some plant operation data recently and found good agreements between our simulation and operation data but we cannot show the comparison in this paper because of some confidentiality issues. We are continuously advancing the transient simulation capability of our program and we expect to present comparisons with real operation data in future publications. Finally, we decided to present comparisons of our program with a commercial program to verify the fundamental modeling of our program. There are only a few commercial programs that are capable of dynamic simulation. For example, PROOSIS provides a similar level of dynamic simulation capability to our program, while GateCycle provides steady state analysis only.

To validate the fundamental thermodynamic modeling of the program, we simulated the transient response of the gas turbine to a load change profile without implementing engine control. The fully controlled simulation will be shown in the next section. Fig. 9 shows the load change profile. The engine is initially at the design point conditions. Then, the input load changes as shown in Fig. 9, and we calculated the engine's response. The actual moment of inertia of the simulated commercial gas turbine is not available. Therefore, we surveyed several sources showing the moment of inertia values for gas turbines that produce similar power output to the simulated engine [37] and used a value of 42000 kgm^2 .

Fig. 10 shows the response of the gas turbine to the load profile of Fig. 9. Figs. 10(a) and (b) show the variations in the simulated power output of the gas turbine and shaft speed. After a small undershoot or overshoot due to the inertia of the shaft, the power output quickly matches the required load. The small peaks in the power and speed caused by abrupt load

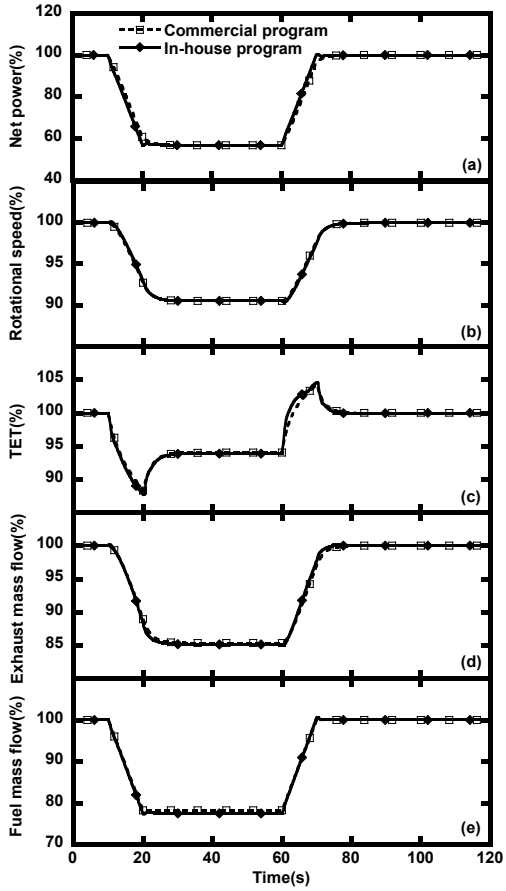

Fig. 10. Response to load profile without engine control: (a) Net power; (b) rotational speed; (c) turbine exhaust temperature; (d) turbine exhaust flow; (e) fuel flow.

changes were captured well by our program. The variations in turbine exhaust temperature, exhaust mass flow rate, and fuel flow are shown in Figs. 10(c)-(e). The turbine exhaust temperature shows a large peak before the power converges to the load. The air and fuel flows follow the load change smoothly. The patterns and numerical values of the simulated results are quite similar to those predicted by PROOSIS, which confirms the validity of the fundamental transient modeling of our program.

3.3 Load-following operation

We next simulated the realistic load-following operation of the gas turbine. The control module described in Sec. 2.8 was applied to analyze the response in accordance with arbitrary load changes. The performance of the PID control depends on the gains in the control equation. Therefore, we selected appropriate gain values via trial and error. Fig. 11 shows an example of the influence of the gains on the simulated result for a stepwise 10 % load reduction. Case 1 is the selected combination of the three gains (K_P, K_I, K_D) that minimizes the deviation of the rotational speed. The results of two other cases with different gain values are also shown for comparison. Table 4

Table 4. Cases with different control gains.

	$K_{P,fuel}$	$K_{I,fuel}$	$K_{D,fuel}$	$K_{P,IGV}$	$K_{I,IGV}$	$K_{D,IGV}$
Case 1	0.0056	$1(10^{-5})$	1.75	$2(10^{-4})$	$1(10^{-5})$	0.4
Case 2	0.008	$1(10^{-5})$	0.4	$1.3(10^{-4})$	$1(10^{-5})$	0.4
Case 3	0.0053	$1(10^{-5})$	0.0016	$1.3(10^{-4})$	$1(10^{-5})$	0.4

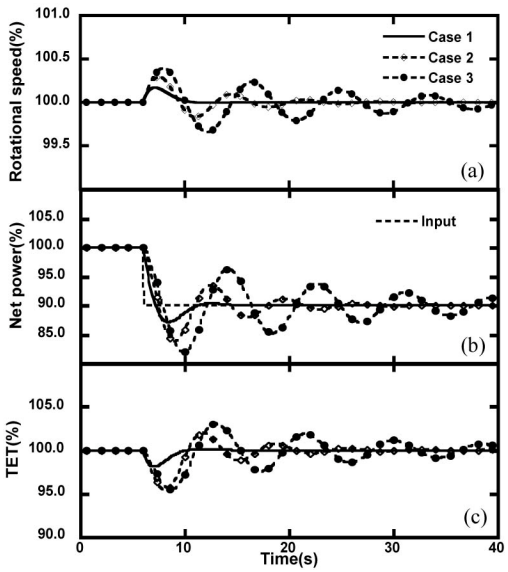

Fig. 11. Simulated parameter changes for a stepwise 10 % load reduction with engine control: (a) Rotational speed; (b) net power; (c) turbine exhaust temperature.

shows the gain values of the three cases.

As shown in Fig. 11, the rotational speed of the optimized case experiences only a single overshoot and rapidly converges to the desired value (3600 rpm), while the other cases show some multiple over- and undershoots and much longer settling time. The overshoot of case 1 is less than 0.2 %. The power output of case 1 converges to the required load in less than 15 seconds. The peak undershoot of the power is less than 2.5 %. The turbine exhaust temperature follows a similar pattern to the power with less than 2 % peak change.

We simulated various load-following operations with the optimal combination of gains (Case 1). We illustrate an example that shows the influences of the magnitude of load change and ramp rate on the dynamic response of the controlled engine. Fig. 12 shows the three different load profiles. The initial conditions are the design conditions. In the first profile, the ramp rate which is the rate of the change of the load input was fixed at 30 MW/min, and the magnitude of the load change was 10 % (17 MW). The same ramp rate was used in the second profile, but the magnitude of load change was increased to 20 % (34 MW). Thus, comparison between the first and second cases showed the influence of the load change magnitude. In the third profile, the magnitude of load change was the same as in the first profile but the ramp rate was reduced to 10 MW/min. 30 MW/min is a typical ramp rate for a fast start-up of F-class gas turbines [38]. Therefore, this value simulates a very rapid load change that represents extreme load-following operating conditions.

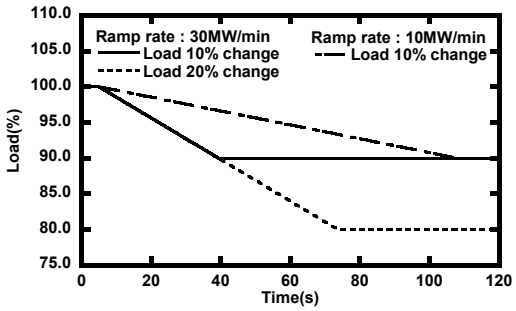

Fig. 12. Three different load profiles for controlled load-following operation.

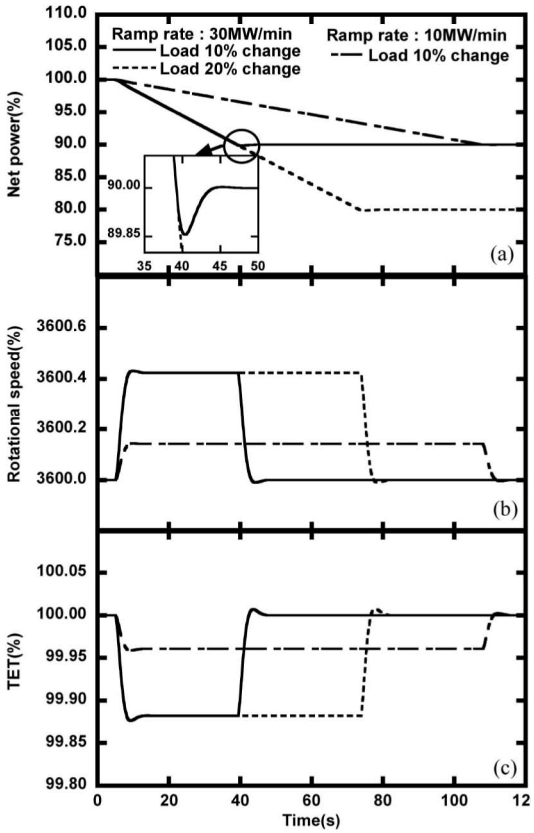

Fig. 13. Response to three different load profiles with engine control: (a) Net power; (b) rotational speed; (c) turbine exhaust temperature.

Fig. 13 shows the response of the gas turbine to the controlled operation followed by the load profiles of Fig. 12. Fig. 13(a) shows the variation in power output. In all cases, the power follows the load very well with only marginal undershoots before settling. The rotational speed increases slightly due to the deceasing load, and the increased shaft speed remains during the load change period, as shown in Fig. 13(b). Then, it returns to the reference speed soon once the load change stops. Fig. 13(c) shows the variation in the turbine

exhaust temperature. The settling time is nearly equivalent among the three parameters. For example, three parameters show the nearly same settling time of about 5 seconds at the end of the 10 % load change with the 30 MW/min rate (see the variations around 40 seconds). The actual partial load operation strategy of the 7FA is to maintain the turbine inlet temperature from base load to 80 % load, as illustrated in Fig. 8. However, we assumed constant turbine exhaust temperature operation to simply illustrate the application of the control logic.

It is clear that the peak increases of the rotational speed and turbine exhaust temperature depend on the ramp rate. The peak of rotational speed is about 0.012 % in the first and second profiles and is further reduced to 0.004 % in the third profile. These peak changes are well within the allowable limit of frequency deviation for electric power plants. This result tells us that the adopted PID controller is very effective for controlling the engine. The exhaust temperature is also controlled very well with peak variation less than 0.15 %, even for the large ramp rate of 30 MW/min.

The results so far show that the dynamic program with the control model would provide physically sound simulation results and could be utilized for simulation of various dynamic operation scenarios in the early stages of engine development.

4. Conclusions

An in-house program for analyzing the dynamic behaviors of heavy-duty gas turbines was developed. Both the multi-stage compressor and turbine were modeled, and the turbine cooling was fully considered. Compressor and turbine performance maps were used. The program can simulate a wide operation range of load and environment conditions without numerical problems.

The transient response of the gas turbine to a typical step-wise load reduction was simulated, and the results were compared with those of a commercial program. The results were quite close, which validated the fundamental thermodynamic modeling of our program.

PID control was used to simulate the simultaneous fuel and IGV controls. An appropriate combination of control gains was obtained by trial and error to make the deviation of the rotational speed sufficiently small. Dynamic responses of the gas turbine under controlled load-following operations were simulated, and the influence of the load change magnitude and ramp rate was examined. Stable control of the gas turbine is possible, even for a very rapid change of load.

This study set up a reliable program to simulate the dynamic operation of heavy-duty gas turbines based on thermodynamic models, component characteristics, and control logic. In the subsequent research, we expect to develop the current program into an extensive version that is capable of simulating start-up and shut-down and predicting the influence of harsh transient operations on gas turbines.

Acknowledgment

This work was supported by the Korea Institute of Energy Technology Evaluation and Planning (KETEP) and the Ministry of Trade, Industry & Energy (MOTIE) of the Republic of Korea (No. 20141010101850).

Nomenclature

A : Area [m^2]
e : Error [-]
f : Fraction of rotor coolant chargeable to power [-]
h : Enthalpy [kJ/kg]
I : Polar moment of inertia [kgm^2]
IGV : Inlet guide vane
K : Gain [-]
$\dot{m}$: Mass flow rate [kg/s]
N : Rotational speed [rpm]
n : Number of stage
LHV : Low heating value [kJ/kg]
P : Pressure [kPa]
PR : Pressure ratio [-]
R : Gas constant [J/kg K]
sf : Scaling factor [-]
T : Temperature [K]
TC : Time constant [s]
TET : Turbine exhaust temperature [K]
TIT : Turbine inlet temperature [K]
TRIT : Turbine rotor inlet temperature [K]
t : Time [s]
$\dot{W}$: Power [MW]
X : Variable [-]
γ : Ratio of specific heat [-]
η : Efficiency [%]
ω : Angular velocity [rad/s]
κ : Constant [$(kJ/kgK)^{-0.5}$]

Subscripts

a,b,c : Locations inside turbine stage
C : Coolant
comp : Compressor
D : Derivative
d : Design point
gen : Generator
I : Integral
in : Inlet
mech : Mechanical
N : Nozzle
o : Original map
out : Outlet
P : Proportional
s : Isentropic
sc : Scaled map
st : Stage

turb : Turbine

References

[1] G. Guandalini, S. Campanari and M. C. Romano, Power to gas plants and gas turbines for improved wind energy dispatchability: Energy and economic assessment, *Applied Energy*, 147 (2015) 117-130.

[2] F. Alobaid, R. Starkloff, S. Pfeiffer, K. Karner, B. Epple and H. G. Kim, A comparative study of different dynamic process simulation codes for combined cycle power plants-Part A: Part loads and off-design operation, *Fuel*, 153 (2015) 692-706.

[3] F. Alobaid, R. Starkloff, S. Pfeiffer, K. Karner, B. Epple and H. G. Kim, A comparative study of different dynamic process simulation codes for combined cycle power plants-Part B: Start-up procedure, *Fuel*, 153 (2015) 707-716.

[4] A. Alexiou, E. H. Baalbergen, O. Kogenhop, K. Mathioudakis and P. Arendsen, Advanced capabilities for gas turbine engine performance simulations, *ASME Paper*, GT2007-27086 (2007).

[5] A. Alexiou and K. Mathioudakis, Development of a turbofan performance model using a generic simulation tool, *ASME Paper*, GT2005-68678 (2005).

[6] H. Asgari, X. Chen, M. Morini, M. Pinelli, R. Sainudiin, P. R. Spina and M. Venturini, NARX models for simulation of the start-up operation of a single-shaft gas turbine, *Applied Thermal Engineering*, 93 (2016) 368-376.

[7] GasTurb GmbH, *GasTurb Ver.12*.

[8] GE Energy, *GateCycle Ver. 6.1.2*.

[9] *NLR - Netherlands Aerospace Centre*, GSP.

[10] Empresarios Agrupados Internacional, *PROOSIS Ver. 3.6.19*.

[11] Trax LLC Energy Solutions, *ProTRAX*.

[12] *Southwest Research Institute*, NPSS.

[13] F. He, Z. Li, P. Liu, L. Ma and E. N. Pistikopoulos, Operation window and part-load performance study of a syngas fired gas turbine, *Applied Energy*, 89 (2012) 133-141.

[14] Y. S. Kim, J. J. Lee, T. S. Kim and J. L. Sohn, Effects of syngas type on the operation and performance of a gas turbine in integrated gasification combined cycle, *Energy Conversion and Management*, 52 (2011) 2262-2271.

[15] J. Y. Kang, D. W. Kang, T. S. Kim and K. B. Hur, Economic evaluation of biogas and natural gas co-firing in gas turbine combined heat and power systems, *Applied Thermal Engineering*, 70 (2014) 723-731.

[16] F. Basrawi, H. Ibrahim and T. Yamada, Optimal unit sizing of biogas-fuelled micro gas turbine cogeneration systems in a sewage treatment plant, *Energy Procedia*, 75 (2015) 1052-1058.

[17] P. P. Walsh and P. Fletcher, *Gas Turbine Performance*, Second Ed., John Wiley & Sons, New Jersey, USA (2004).

[18] Mathworks, *MATLAB R2012b*.

[19] R. K. Agrawal and M. Yunis, A generalized mathematical model to estimate gas turbine starting characteristics, *ASME J. of Engineering for Power*, 104 (1982) 194-201.

[20] H. I. H. Saravanamuttoo and B. D. MacIsaac, The use of a hybrid computer in the optimization of gas turbine control parameters, *ASME J. of Engineering for Power*, 95 (1973) 257-264.

[21] National Institute Standards and Technology, *REFPROP Ver. 9.1*.

[22] R. E. Sonntag and G. J. V. Wylen, *Introduction to Thermodynamics: Classical and Statistical*, Third Ed., John Wiley & Sons, New Jersey, USA (1991) 729-730.

[23] J. J. Lee, D. W. Kang and T. S. Kim, Development of a gas turbine performance analysis program and its application, *Energy*, 36 (2011) 5274-5285.

[24] GasTurb GmbH, *Smooth C Ver. 8.2* (2001).

[25] S. R. Turns, *An Introduction to Combustion: Concepts and Applications*, Second Ed., McGraw-Hill, New York, USA (2000).

[26] C. A. Palmer and M. R. Erbes, Simulation methods used to analyze the performance of the GE PG6541B gas turbine utilizing low heating value fuels, *ASME Cogen Turbo Power* (1994) 1-10.

[27] J. F. Dugan Jr., Aerodynamic design of axial-flow compressors, *NASA SP-36* (1965) Chapter XVII.

[28] H. I. H. Saravananmuttoo, G. F. C Rogers and H. Cohen, *Gas Turbine Theory*, Fifth Ed., Prentice Hall, New Jersey, USA (2001).

[29] J. H. Kim, T. W. Song, T. S. Kim and S. T. Ro, Model development and simulation of transient behavior of heavy duty gas turbines, *J. of Engineering for Gas Turbines and Power*, 123 (2001) 589-594.

[30] M. M. Carrero, M. L. Ferrari, W. D. Paepe, A. Parente, S. Bram and F. Contino, Transient simulations of a T100 micro gas turbine converted into a micro humid air turbine, *ASME Paper,* GT2015-43277 (2015).

[31] M. J. Kim, J. H. Kim and T. S. Kim, Program development and simulation of dynamic operation of micro gas turbines, *Applied Thermal Engineering*, 108 (2016) 122-130.

[32] S. C. Chapra and R. P. Canale, *Numerical Methods for Engineers*, Sixth Ed., McGraw-Hill, New York, USA (2010).

[33] R. Eldrid, L. Kaufman and P. Marks, The 7FB: the next evolution of the F gas turbine, *General electric report*, GER-4194.

[34] R. Farmer, *Gas turbine world handbook*, Pequot Publishing Inc., North Carolina, USA (2007).

[35] B. J. McBride and S. Gordon, *Computer Program for Calculation of Complex Chemical Equilibrium Compositions and Applications I. Analysis*, NASA Reference Publication, NASA RP-1311 (1994).

[36] F. J. Brooks, GE gas turbine performance characteristics, *General electric report*, GER-3567H .

[37] *http://www.energy.ca.gov/sitingcases/redondo_beach/documents/applicant/AFC/Vol_2/RBEP_Appendix%203A_CAISO%20Interconnection%20Request%20and%20Payment.pdf.*

[38] *https://powergen.gepower.com*.

J. H. Kim received his M.S. degree from Dept. of Mechanical Engineering, Inha University in 2014, and is now a doctoral student in the same department. His major research topic is simulation of gas turbine operation.

T. S. Kim received his Ph.D. degree from Dept. of Mechanical Engineering, Seoul National University in 1995. He has been with Dept. of Mechanical Engineering, Inha University since 2000. His research interests are design and analysis of advanced energy systems including gas/steam turbine based power plants.

S. J. Moon received his Ph.D. degree from Dept. of Mechanical Engineering, U.C. Berkeley in 2001. He has been with Dept of Mechanical Engineering, Hanyang University since 2003. His research interests are combined-cycle power plant simulation, graphene and micro/nano scale engineering including E-ink laser sintering, a-si laser crystallization and LIBS.